Published in final edited form as:
*Neurobiol Aging*. 2012 September ; 33(9): 2091–2105. doi:10.1016/j.neurobiolaging.2011.09.024.

# Multimodality Imaging Characteristics of Dementia with Lewy Bodies

**Kejal Kantarci, MD, MSC**[1,*], **Val J. Lowe, MD**[1], **Bradley F. Boeve, MD**[2], **Stephen D. Weigand, MS**[3], **Matthew L. Senjem, MS**[1], **Scott A. Przybelski, BS**[3], **Dennis W. Dickson, MD**[4], **Joseph E. Parisi, MD**[5], **David S. Knopman, MD**[2], **Glenn E. Smith, PhD**[6], **Tanis J. Ferman, PhD**[7], **Ronald C. Petersen, MD, PhD**[2], and **Clifford R. Jack Jr, MD**[1]

[1]Department of Radiology, Mayo Clinic, Rochester, Minnesota

[2]Department of Neurology, Mayo Clinic, Rochester, Minnesota

[3]Department of Health Sciences Research, Mayo Clinic, Rochester, Minnesota

[4]Departments of Pathology and Laboratory Medicine and Neuroscience, Mayo Clinic, Jacksonville, Florida

[5]Department of Pathology and Laboratory Medicine, Mayo Clinic, Rochester, Minnesota

[6]Department of Psychiatry and Psychology, Mayo Clinic, Rochester, Minnesota

[7]Department of Psychiatry and Psychology, Mayo Clinic, Jacksonville, Florida

## Abstract

Dementia with Lewy bodies (DLB) is the second most common cause of neurodegenerative dementia after Alzheimer's disease (AD). Our objective was to determine whether the $^{11}$C–Pittsburgh Compound-B (PiB) retention and regional hypometabolism on PET and regional cortical atrophy on MRI are complementary in characterizing patients with DLB and differentiating them from AD. We studied age, gender and education matched patients with a clinical diagnosis of DLB (n=21), AD (n=21), and cognitively normal subjects (n=42). Hippocampal atrophy, global cortical PiB retention and occipital lobe metabolism in combination distinguished DLB from AD better than any of the measurements alone (area under the receiver operating characteristic=0.98).Five of the DLB and AD patients who underwent autopsy were distinguished through multimodality imaging. These data demonstrate that MRI and PiB PET contribute to characterizing the distinct pathological mechanisms in patients with AD compared to DLB. Occipital and posterior parietotemporal lobe hypometabolism is a distinguishing feature of DLB and this regional hypometabolic pattern is independent of the amyloid pathology.



[*]**Corresponding Author:** Kejal Kantarci, MD, Mayo Clinic, 200 First Street SW, Rochester, MN 55905, **Phone:** 507- 284 9770, **Fax:** 507-284 9778, kantarci.kejal@mayo.edu.



**Disclosure Statements**

The authors do not have any actual or potential conflicts of interests to disclose. This study was approved by the Mayo Clinic Institutional Review Board, and informed consent for participation was obtained from every subject and/or an appropriate surrogate.

**Keywords**

Dementia with Lewy bodies; MRI; PET; FDG; PiB; Alzheimer's disease

## Introduction

Dementia with Lewy bodies (DLB) is the second most common cause of neurodegenerative dementia after Alzheimer's disease (AD) [Barker, et al.,2002, [Galasko, et al.,1994,Joachim, et al.,1988,Zaccai, et al.,2005]. Although the mechanisms of pathogenesis in AD and DLB are different, many patients with DLB have a varying degree of AD pathology in addition to Lewy related pathology (LRP) [Fujishiro, et al.,2010,Galasko, et al.,1994,Gomez-Tortosa, et al.,1999,Hansen, et al.,1990,[Schneider, et al.,2007]. The diagnostic accuracy for DLB based upon postmortem confirmation is relatively low [Luis, et al.,1999,McKeith, et al., 2000,Merdes, et al.,2003,Verghese, et al.,1999], improved with the revised criteria of the Third International Workshop on DLB in 2005 [Fujishiro, et al.,2008,McKeith, et al.,2005], but still imperfect. The challenge of clinical diagnosis in patients with AD and DLB stems from the fact that the underlying pathology is frequently complex with contribution from both AD and LB disease pathologies [McKeith, et al.,2005]. The potential for disease-modifying treatments for AD, as well as the responsiveness to cholinesterase inhibitor treatment and marked neuroleptic sensitivity of DLB patients generate a need for surrogate markers for AD and LB disease pathologies for accurate diagnosis [Quigley, et al.,2010].

A majority of patients with DLB are pathologically characterized by the presence of β-amyloid (Aβ) deposition. In keeping with that, *in vivo* PET amyloid labeling tracer [N-methyl-11C]2-(40-methylaminophenyl)-6-hydroxybenzothiazole also known as $^{11}$C-Pittsburgh Compound B (PiB) binding is typically present in up to 80% of patients with DLB, although at lower levels than in AD [Edison, et al.,2008,Foster, et al.,2010,Gomperts, et al.,2008,Maetzler, et al.,2009]. Cortical PiB binding in DLB is largely attributable to the binding to Aβ and not to α-synuclein-containing Lewy bodies [Burack, et al.,2010,Fodero-Tavoletti, et al.,2007,Kantarci, et al.,2010,Ye, et al.,2008], and the specificity of *in vivo* PiB binding to Aβ has been confirmed at autopsy in a case with DLB (Kantarci et al., 2010). Although amyloid deposition is central to the pathology of AD, it does not correlate with cognitive function as well as the neurofibrillary pathology of AD [Dickson, et al., 1995,Giannakopoulos, et al.,1994,Gomez-Isla, et al.,1997,Grober, et al.,1999,Guillozet, et al.,2003,Nagy, et al.,1995]. Furthermore, diffuse amyloid plaques, which are a common in patients with DLB [Dickson,2002], but not a diagnostic feature of AD [The National Institute on Aging 1997] contribute to PiB retention in LB diseases [Burack, et al., 2010,Kantarci, et al.,2010]. The distinction between neuritic and diffuse plaques however is not possible with PiB PET, since PiB labels both neuritic and diffuse plaques, although labeling of diffuse/amorphous plaques is less prominent than compact/cored plaques [Ikonomovic, et al.,2008,Lockhart, et al.,2007,Sojkova, et al.]. Therefore, brain amyloid load on amyloid ligand PET imaging by itself is insufficient for determining presence of neuritic plaques in patients with DLB.

A structural imaging correlate of neurodegeneration accompanying the neurofibrillary pathology of AD is cortical atrophy [Barkhof, et al.,2007,Bobinski, et al.,1997,Csernansky, et al.,2004,Gosche, et al.,2002,Jack, et al.,2002,Jagust, et al.,2008,Silbert, et al., 2003,Vemuri, et al.,2010,Whitwell, et al.,2008,Zarow, et al.,2005]. MRI-pathology correlation studies have shown that the severity of hippocampal atrophy correlates well with Braak stage [Gosche, et al.,2002,Jack, et al.,2002] and with the neurofibrillary tangle density [Csernansky, et al.,2004,Silbert, et al.,2003,Vemuri, et al.,2008,Whitwell, et al.,2008]. Excellent correlation was found between hippocampal volume measures obtained on either

antemortem MRI [Zarow, et al.,2005] or postmortem MRI [Bobinski, et al.,1997] and hippocampal neuron cell counts in autopsy specimens. Hippocampal atrophy was a distinguishing feature of AD compared to DLB in clinically diagnosed cohorts [Burton, et al.,2002,Firbank, et al.,2010,Whitwell, et al.,2007] and autopsy confirmed cases [Burton, et al.,2009,Burton, et al.,2011,Kantarci, et al.,2011].

While PiB PET and structural MRI may be useful in detecting the pathological features of AD, patients with DLB are characterized by hypometabolism in the parietal and occipital cortex on [$^{18}$F]2-fluoro-deoxy-D-glucose (FDG) PET images. Occipital lobe hypometabolism differentiates patients with DLB from AD in both clinically diagnosed [Imamura, et al.,1997,Ishii, et al.,1998,Mosconi, et al.,2008,Teune, et al.], and in autopsy confirmed [Albin, et al.,1996,Higuchi, et al.,2000,Minoshima, et al.,2001] cohorts. Furthermore, occipital hypometabolism is associated with visual hallucinations in DLB [Imamura, et al.,1999,Perneczky, et al.,2008]. The metabolic impairment in the occipital lobe responds to cholinesterase treatment [Mori, et al.,2006,Satoh, et al.,2010], suggesting a link between cholinergic dysfunction [Shimada, et al.,2009], clinical symptoms and occipital lobe hypometabolism in DLB.

Our objective was to determine structural MRI, PiB PET and FDG PET imaging characteristics of patients with DLB. The rationale for investigating multi-modality imaging lies in the multi-factorial nature of pathological involvement in many patients with DLB. Structural MRI is a surrogate for the neuronal degeneration and PiB PET is a direct measure of the Aβ pathology. Finally, specific patterns of FDG PET glucose hypometabolism have been associated with LRP. We hypothesized that the three imaging modalities that are sensitive to different components of the disease process would provide complementary information for characterizing patients with DLB and differentiating patients with DLB from AD.

## Methods

### Subjects

This study included 21 consecutive patients with DLB who were recruited from the Mayo Clinic Alzheimer Disease Research Center (ADRC), met the Third Report of the DLB Consortium criteria for probable DLB [McKeith, et al.,2005] and participated in the PET and MRI studies from April 2006 through February 2011. We identified 21 patients with AD who met the NINCDS-ADRDA criteria for probable AD [McKhann, et al.,1984] and 42 cognitively normal (CN) subjects from the ADRC and Mayo Clinic Study of Aging [Roberts, et al.,2008], which is a longitudinal population-based cohort. AD subjects were matched to DLB patients (1:1) and CN subjects were matched to DLB patients (2:1) on age, gender and education. Exclusion criteria were: 1) presence of structural abnormalities that could cause cognitive impairment or dementia such as brain tumors 2) concurrent illnesses or treatments interfering with cognitive function other than AD or DLB.

Informants and patients were interviewed regarding temporal onset and frequency of symptoms. Clinical features of DLB was recorded using the following criteria: 1) Presence and severity of parkinsonism was rated with the Unified Parkinson's Disease Rating Scale (UPDRS); 2) Visual hallucinations were fully formed, occurring on more than one occasion and not attributable to medical factors (e.g. infection, postoperative confusion), medications or advanced dementia. The frequency of visual hallucinations were rated on a 4 point scale (1= <1 per week, 2= one per week, 3=several per week, 4=daily) 3) Fluctuations were considered present if the patient scored 3 or 4 on the Mayo Fluctuations Questionnaire [Ferman, et al.,2004]; 4) Patients with probable REM sleep behavior disorder (pRBD) met the International Classification of Sleep Disorders-II diagnostic criteria B for pRBD

[AASM,2005]. All subjects underwent clinical evaluation, PET and MRI studies within a five month period. The median (range) time between MRI/PET scanning and clinical evaluation was 2.0 (1.7, 4.4) months.

### MRI Acquisition

MRI examinations were performed at 3 Tesla using an eight-channel phased array coil (GE, Milwaukee, WI). A 3D high resolution MPRAGE acquisition with TR/TE/TI = 7/3/900 ms; flip angle 8 degrees; in plane resolution of 1.0 mm and a slice thickness of 1.2 mm was performed for anatomical segmentation and labeling.

### $^{11}$C-PiB PET and $^{18}$F-FDG PET Acquisitions

PET images were acquired using an LYSO PET/CT scanner (DRX; GE Healthcare) operating in 3-dimensional mode. A computerized tomography image was obtained for attenuation correction. Subjects were injected with both $^{11}$C-PiB (average, 596 MBq; range, 292–729 MBq) and $^{18}$F-FDG (average, 540 MBq; range, 366–399 MBq). The images were acquired on the same day, with 1 hour between the $^{11}$C-PiB and $^{18}$F-FDG PET scan acquisitions. Following a 40 min $^{11}$C-PiB uptake period, a 20 min $^{11}$C-PiB scan was obtained. $^{11}$C-PiB PET acquisition consisted of four 5 min dynamic frames, acquired from 40 to 60 min after injection. Following a 30 min $^{18}$F-FDG uptake period, an 8 min$^{18}$F-FDG scan was obtained. Image acquisition consisted of four 2-min dynamic frames, acquired from 30 to 38 min after injection. Standard corrections were applied.

### Structural MRI Analysis

The automated anatomic labeling (AAL) atlas [Tzourio-Mazoyer, et al.,2002] was manually modified in-house on a cognitively normal older subject's high-resolution T1 weighted MRI [Kantarci, et al.,2010]. Atlas labels were then normalized to the custom template generated from 200 AD and 200 controls [Vemuri, et al.,2008] using the unified segmentation method in Statistical Parametric Mapping (SPM)5 [Ashburner and Friston,2005] giving a set of labels corresponding to the custom template space. Between-group differences in grey matter density were assessed using a two-sided t-test within the general linear model framework of SPM5. Statistical maps of group differences were displayed at a significance value of $P<0.05$, using family-wise error (FWE) correction for multiple comparisons. The resulting subject specific atlas was used to parcellate grey matter images into the modified AAL atlas regions of interest (ROI) in the subject's T1 image space. The normalized ROI volumes were divided by the total intracranial volume.

### PET Image Analysis

PiB PET and FDG PET image volumes of each subject were co-registered to his/her own T1-weighted MRI scan with the modified AAL atlas labels, using a 6-degrees of freedom affine registration with mutual information cost function. Atlas-based parcellation of FDG and PiB PET images into ROIs was therefore performed in subject's T1-weighted MRI space. Partial volume correction for tissue and cerebrospinal fluid (CSF) compartments was applied using the two compartment model [Meltzer, et al.,1999] to remove atrophy effects on the FDG and PiB uptake on PET images. Cerebellar uptake was used as an internal reference ROI for PiB PET normalization and pons was used as an internal reference ROI for FDG PET normalization to calculate FDG and PiB PET ratio images. Voxel-wise PiB and FDG uptake differences between groups were assessed using a two-sided T-test within the general linear model framework of SPM5. Statistical maps of group differences were displayed at a significance value of $P<0.05$, using FWE correction for multiple comparisons. Statistics on image voxel values were extracted from modified AAL atlas ROIs . The median value in each target cortical ROI was divided by the median value in the

cerebellar ROI for PiB PET and pontine ROI for FDG PET images. The global cortical PiB retention ratio was calculated by averaging the PiB retention ratio from the bilateral parietal (including posterior cingulate and precuneus), temporal, prefrontal, orbitofrontal, anterior cingulate grey matter regions where the average is weighted by ROI size [Jack, et al., 2007,Lowe, et al.,2009].

### Statistical Analysis

Because neither AD nor DLB pathologies differentially involve either hemisphere, right and left hemispheric values were weighted averaged for PET measurements and summed for the volumetric measurements for statistical analysis. We performed a chi-squared test of differences in gender distribution across groups and used a Kruskal-Wallis test to evaluate whether there were systematic differences in age and education across groups. We compared patient groups on numeric clinical measures and quantitative imaging markers using pairwise Wilcoxon rank-sum/Mann-Whitney U-tests. We used single variable and multivariable logistic regression models to compare imaging markers for distinguishing patients with AD and DLB and to investigate whether each imaging marker independently contributes to distinguishing the two patient groups. We summarize how well the markers discriminate alone or on combination with Harell's C-statistic which is equivalent to area under the receiver operating characteristic curve (AUROC) [Harrell,2001]. Spearman rank-order correlation test was used to investigate the association between the imaging measurements and UPDRS, duration of fluctuations, pRBD parkinsonism, and the duration and frequency of visual hallucinations as. All analyses were performed using R version 2.11.0 and Harrell's Design package.

## Results

### Subject characteristics

Characteristics of the study subjects are listed in Table 1. Owing to the matching performed, AD, DLB and CN groups had similar demographic features. Functional dementia severity measured with Clinical Dementia Rating Sum of Boxes (CDR SOB) was not different among AD and DLB patients. A majority of DLB patients had fluctuations (62%; median duration=3.6 years), visual hallucinations (90%; median duration=2.2 years), parkinsonism (90%; median duration=2.2 years) and pRBD (90%; median duration=9.7 years). Because only a small number of patients with DLB did not have visual hallucinations (n=2), parkinsonism (n=2) or pRBD (n=2), we could not compare the imaging findings in DLB patients with and without visual hallucinations, parkinsonism and pRBD. On the other hand, we were able to test for the associations between imaging findings and presence of fluctuations and UPDRS and the frequency of visual hallucinations (median frequency score = 3 (several times per week but less than daily)) in patients with DLB.

### Structural MRI findings distinguishing patients with AD and DLB

Voxel-based analysis showed smaller hippocampal volumes in patients with AD compared to patients with DLB ($P<0.05$; FWE corrected for multiple comparisons) (Figure 1) Cortical grey matter density of patients with DLB was not different from the CN subjects ($P<0.05$; FWE corrected for multiple comparisons). Patients with AD had smaller hippocampal volumes compared to patients with DLB and CN subjects on ROI analysis ($p<0.001$). No difference in hippocampal volumes were observed between patients with DLB and CN subjects ($p=0.93$). We did not find any association between hippocampal volumes and UPDRS, CDR SOB, frequency of visual hallucinations and the duration of clinical features in patients with DLB ($p>0.25$). There were no differences in hippocampal volumes between DLB patients with and without fluctuations ($p=0.86$).

### PiB PET findings in patients with DLB

The global cortical PiB retention ratio in patients with DLB was lower than patients with AD ($p<0.001$) but higher than the CN subjects ($p=0.03$). According to the typically used cut-off of 1.50 [Jack, et al.,2008,Rowe, et al.,2007], 11 out of 21 (52%; 95% confidence interval= 30%-74%) of the patients with DLB were classified as PiB-positive. There were four DLB patients (three PiB-negative and one PiB-positive) and two AD patients who had borderline PiB retention (global cortical PiB retention ratio = 1.4 – 1.6). On the other hand, only 9 out of 42 (21%; 95% confidence interval= 11%– 37%) CN subjects were classified as PiB positive.

In order to determine the topography of increased cortical PiB retention in DLB, we performed voxel-based analysis comparing patients with DLB to CN subjects and found no differences between the two groups ($P<0.05$; FWE corrected for multiple comparisons). Because 48% of DLB patients were PiB-negative and 21% of the CN patients were PiB-positive, in a secondary analysis, we excluded these cases and compared PiB-positive patients with DLB (n=11) to PiB-negative CN subjects (n=33). The topography of PiB distribution in PiB-positive patients with DLB involved the medial frontal, prefrontal, lateral parietal, superior temporal, cingulate gyrus and precuneus regions; but not the occipital lobe, pre and post central gyri, medial and inferior temporal lobe cortices ($P<0.05$; FWE corrected for multiple comparisons) (Figure 2). We did not find any association between global cortical PiB retention and UPDRS, CDR SOB, frequency of visual hallucinations and the duration of clinical features in patients with DLB ($p>0.08$). There were no differences in global cortical PiB retention between DLB patients with and without fluctuations ($P=0.75$).

### FDG PET findings in patients with DLB

Patients with DLB had lower FDG uptake in the parietal, occipital and posterior temporal lobes compared to CN subjects on voxel-based analysis ($P<0.05$; FWE corrected for multiple comparisons). In order to determine whether Aβ load influence the FDG reduction in patients with DLB, we stratified DLB patients into PiB-positive (n=11) and PiB-negative (n=10) groups. We found no difference between the FDG uptake in PiB-positive compared to PiB-negative patients with DLB. When PiB positive and PiB negative DLB patients were compared to PiB negative CN subjects, occipital and posterior parietotemporal lobe hypometabolism was identified both in PiB-positive and PiB-negative patients with DLB ($P<0.05$; FWE corrected for multiple comparisons) (Figure 3). We did not find any association between occipital FDG uptake and UPDRS, CDR SOB, and the duration of visual hallucinations, fluctuations and parkinsonism in patients with DLB ($p>0.22$). There was an association between the occipital FDG uptake and the frequency of visual hallucinations ($rho=-0.66$; $p=0.01$) and a trend of an association with the duration of pRBD ($rho=-0.42$; $p=0.06$). Occipital FDG uptake was lower in DLB patients with fluctuations compared to DLB patients without fluctuations ($p=0.04$).

FDG uptake in the occipital lobe, posterior temporal, posterior parietal and posterior precuneus regions were lower in patients with DLB compared to patients with AD ($P<0.05$; FWE corrected for multiple comparisons). A majority of the clusters were within the occipital lobe (Figure 4). Patients with DLB had significant reduction in the occipital lobe FDG uptake and increased posterior cingulate to the sum of the precuneus plus cuneus FDG uptake ratio (i.e. cingulate island sign [Lim, et al.,2009]) compared to patients with AD and CN subjects on ROI analysis ($p<0.001$).

## Complementary role of multi-modality imaging in distinguishing patients with DLB from AD

The ROI-based and voxel-based analysis showed that hippocampal volumes on structural MRI, global cortical PiB retention and occipital lobe hypometabolism on PET were useful in distinguishing patients with DLB and AD. On univariate logistic regression models, each of the quantitative imaging markers were comparable in accuracy for distinguishing patients with DLB and AD. Including two of the imaging markers in the model improved the area under the ROC (AUROC) curve for distinguishing patients with AD and DLB. All three imaging markers contributed significantly to the bivariate logistic regression models ($p<0.05$). The three-marker logistic regression model only slightly improved the accuracy for distinguishing patients with AD and DLB with modest independent contributions from each of the imaging modalities (AUROC=0.98; $P\leq0.05$) (Table 2). Figure 5 shows the plots separating the AD and DLB patients by combining the information from two imaging markers. Figure 6 shows the plots separating the AD and DLB patients by combining the information from all three imaging markers.

We performed a secondary analysis by replacing occipital lobe FDG uptake with the posterior cingulate to precuneus plus cuneus FDG uptake ratio that was proposed as an accurate marker for distinguishing AD and DLB [Lim, et al.,2009]. Although this ratio distinguished patients with AD and DLB with a higher AUROC (0.92) compared to the occipital FDG uptake (0.84) on univarate logistic regression models, the two measures were comparable in distinguishing patients with AD and DLB when multiple modalities were considered.

## Autopsy findings in five cases

Five of the cases in the AD (n=2) and DLB (n=3) cohorts of the current study had autopsy. The characteristics of each subject, imaging and pathologic findings are listed in Table 3. These cases are labeled on the scatter plots showing the imaging findings in Figure 5.

**Case 1** was an 82-year-old man who was clinically diagnosed with probable AD and had a CDR SOB of 13 at the time of imaging studies. The patient died 10 months after the PET and MRI exams. The diagnosis at autopsy was high likelihood of AD according to the NIA-Reagan criteria [Hyman and Trojanowski,1997] with Braak stage VI [Braak and Braak, 1991] neurofibrillary pathology and frequent neuritic plaques [Mirra, et al.,1991]. In agreement with the pathologic diagnosis, this patient had significant hippocampal atrophy and high global cortical PiB retention ratio. Occipital FDG uptake was as low as in patients with DLB even though this patient did not have LB disease. It was possible to distinguish Case 1 from the patients with DLB by combining hippocampal volumes and PiB retention.

**Case 2** was an 88-year-old man who was clinically diagnosed with probable AD. He had a CDR SOB of 7 at the time of imaging studies. The patient died 11 months after the PET and MRI exams. The diagnosis at autopsy was hippocampal argyrophilic grain disease and low likelihood of AD with Braak stage II neurofibrillary pathology and sparse neuritic plaques. In agreement with the pathological diagnosis of low likelihood of AD and hippocampal argyrophilic grain disease, this patient had moderate hippocampal atrophy, low global cortical PiB retention ratio and normal occipital FDG uptake. It was possible to distinguish Case 2 from the patients with DLB by combining hippocampal volumes and occipital FDG uptake.

**Case 3** was an 81-year-old man who had all the core clinical features of DLB and pRBD, was clinically diagnosed with probable DLB and had a CDR SOB of 6 at the time of imaging studies The patient died 11 months after the PET and MRI exams. The diagnosis at

autopsy was high likelihood of DLB according to the Third Report of the DLB Consortium criteria [McKeith, et al.,2005] with limbic (transitional) LRP and low likelihood of AD according to the NIA-Reagan criteria with Braak stage III neurofibrillary pathology and sparse neuritic plaques. In agreement with the pathological diagnosis of high likelihood of DLB, this patient had mild hippocampal atrophy, borderline global cortical PiB retention ratio but significantly low occipital FDG uptake. It was possible to distinguish Case 3 from patients with AD by combining any of the two imaging markers.

**Case 4** was a 75-year-old man who had two of the core clinical features of DLB (parkinsonism and visual hallucinations) and pRBD, was clinically diagnosed with probable DLB and had a CDR SOB of 2.5 at the time of imaging studies. The patient died 17 months after the PET and MRI exams. The diagnosis at autopsy was high likelihood of DLB according to the Third Report of the DLB Consortium criteria with diffuse LRP and low likelihood of AD according to the NIA-Reagan criteria with Braak stage II neurofibrillary pathology and moderate neuritic plaques. This patient had mild hippocampal atrophy, borderline cortical PiB retention ratio and moderately low occipital FDG uptake. It was possible to distinguish Case 4 from the patients with AD by combining any of the two imaging markers.

**Case 5** was previously published in a imaging pathology correlation study by using ROI based methods to demonstrate the specificity of PiB to Aβ in DLB [Kantarci, et al.,2010]. The case was a 75-year-old man who had all the core clinical features of DLB and pRBD, was clinically diagnosed with probable DLB and had a CDR SOB of 5 at the time of imaging studies. The patient died 18 months after the PET and MRI exams. The diagnosis at autopsy was high likelihood of LB disease according to the Third Report of the DLB Consortium criteria with diffuse LRP and low likelihood of AD according to the NIA-Reagan criteria with Braak stage III neurofibrillary pathology and sparse neuritic plaques but frequent diffuse plaques. This patient had mild hippocampal atrophy, high cortical PiB retention ratio but significantly low occipital FDG uptake. It was possible to distinguish Case 5 from AD patients by combining any of the two imaging markers.

## Discussion

This study demonstrates the characteristic pattern of structural MRI, FDG and PiB PET changes in patients with DLB compared to AD. The imaging markers of specific pathophysiological processes, including neurofibrillary pathology/neuronal loss, amyloid deposition and LRP related hypometabolism were useful in characterizing patients with DLB. Hippocampal atrophy and increased global cortical PiB retention, which are associated with neurofibrillary pathology/neuronal loss and amyloid deposition in AD, and occipital hypometabolism which is typically associated with LRP, were complementary in distinguishing patients with AD and DLB.

### Structural MRI findings distinguishing patients with AD and DLB

We did not find any cortical atrophy in patients with DLB and preservation of the hippocampal volume was the characteristic structural MRI finding that distinguished patients with DLB from AD. The structural MRI changes identified in clinically diagnosed patients with DLB have been variable [Barber, et al.,1999,Burton, et al.,2002,Tam, et al., 2005,Whitwell, et al.,2007], which may due to the variable presence of concomitant AD pathology in clinically diagnosed patients with DLB [Kantarci, et al.,2011]. Several studies have reported temporal and frontal lobe atrophy [Barber, et al.,1999,Burton, et al., 2002,Tam, et al.,2005] but we did not find cortical atrophy in a separate cohort of clinically diagnosed patients with DLB [Whitwell, et al.,2007]. Medial temporal lobe or hippocampal atrophy was a distinguishing feature of AD compared to DLB both in clinically diagnosed

patients [Sabattoli, et al.,2008,Whitwell, et al.,2007], and in pathologically confirmed cases [Burton, et al.,2009,Burton, et al.,2011,Kantarci, et al.,2011,Lippa, et al.,1998]. Recently, using three-dimensional parametric surface mesh models, tissue loss was reported in the anterior sector of CA1 in clinically diagnosed patients with DLB compared to patients with AD [Sabattoli, et al.,2008]. Another study however found that subiculum thickness and CA1 area was significantly lower in AD compared to DLB on high resolution MRIs [Firbank, et al.,2010]. Although we did not perform hippocampal shape analysis, the VBM findings in our cohort suggest that the hippocampal volume differences between patients with AD and DLB may involve the posterior portion of the hippocampus more than the anterior (Figure 1). This variation in regional hippocampal volume difference among AD and DLB patients may be due to different regional vulnerability of hippocampus in AD and DLB [Dickson, et al.,1991], which requires further investigations in pathologically confirmed cases.

### PiB Retention in Patients with DLB

In the current study, more than half (52%; 95% confidence interval= 30%– 74%) of the patients with DLB were PiB-positive. This is comparable to [Edison, et al.,2008,Foster, et al.,2010,Maetzler, et al.,2009] or lower [Gomperts, et al.,2008] than the rate of PiB positivity previously reported in smaller DLB cohorts. Higher Aβ load did not have an impact on cognitive functional impairment measured with CDR SOB or motor impairment measured with UPDRS in patients with DLB. The regional pattern of PiB retention in patients with DLB who were PiB-positive reflected the pattern typically seen in patients with AD involving the frontal, parietal and superior temporal lobe association cortices. Occipital, inferior and medial temporal lobes and the primary sensory-motor cortices were relatively spared. Increased striatal PiB retention has been reported in patients with DLB [Edison, et al.,2008] and Aβ pathology has been identified in DLB and Parkinson disease with dementia at autopsy [Fujishiro, et al.,2010,Kalaitzakis, et al.,2011]. In contrast, we did not find increased striatal PiB retention on voxel-based analysis in PiB-positive patients with DLB.

We note that one of the PiB-positive and three of the PiB negative patients with DLB had borderline PiB retention (global cortical PiB retention ratio=1.4–1.6) overlapping with two of the AD patients who also had borderline PiB retention. Of these patients with borderline PiB retention, one AD (Case 2) and two DLB patients (Cases 3 and Case 4) had autopsy. The neuritic plaques in these patients were sparse to moderate and they had Braak stage II-IV neurofibrillary pathology. If Case 3 and Case 4 did not have additional LRP, they would have been classified as low likelihood of AD. Although global cortical PiB retention in a patient with dementia can be classified as positive or negative for diagnostic practicality, it is important to note that Aβ deposition is a continuous pathological process and so is PiB retention. Our data suggest that borderline PiB retention ratio especially in patients with DLB may be an important marker for sparse or moderate neuritic plaques and low or intermediate likelihood of AD pathology.

Contrary to the low or intermediate likelihood of AD pathology in cases with borderline PiB retention one of the PiB positive patients with DLB (Case 5) was pathologically diagnosed as low likelihood of AD because the case had sparse neuritic plaques and Braak III neurofibrillary pathology. In this case, diffuse plaques were on average 2 to 3 times more abundant than the neuritic plaques on modified Bielschowsky silver stain in cortical regions that contributed to the PiB retention [Kantarci, et al.,2010]. A similar observation was reported in two cases with Parkinson disease with dementia who were PiB positive with a high burden of diffuse plaques, but had a low likelihood of AD according to NIA-Reagan criteria at autopsy [Burack, et al.,2010]. Diffuse plaques are common in Lewy body disorders [Dickson,2002] and likely contribute to the PiB retention [Burack, et al., 2010,Kantarci, et al.,2010]. Determining the relationship between diffuse plaques and

cognitive impairment in DLB will be important for making treatment decisions especially for potential treatments with anti-amyloid agents.

## FDG PET findings in patients with DLB compared to patients with AD and CN subjects

Patients with DLB had significant occipital and posterior parietotemporal hypometabolism compared to CN subjects, in agreement with previous studies in DLB [Albin, et al., 1996,Higuchi, et al.,2000,Imamura, et al.,1997,Minoshima, et al.,2001,Mosconi, et al., 2008,Teune, et al.,2010]. In the current study, we showed for the first time that this specific pattern of hypometabolism in patients with DLB is independent of Aβ load. Both PiB-positive and PiB-negative patients with DLB were characterized by hypometabolism in the occipital and posterior parietotemporal lobes. In theory, presence of Aβ pathology in DLB may have an impact on the FDG metabolism in regions with significant Aβ load such as the frontal lobes. However, we found no evidence of a difference in frontal lobe FDG hypometabolism in DLB patients with high Aβ load compared to low Aβ load. Our data suggests that the occipital and posterior parietotemporal hypometabolism observed in patients with DLB is associated with LRP and is not influenced by the presence of Aβ pathology that is common in patients with DLB. The pathological mechanism underlying profound FDG PET hypometabolism in patients with DLB does not appear to be Aβ but may possibly be synaptic dysfunction [Rocher, et al.,2003] due to presynaptic a-synuclein deposition with loss of postsynaptic dendritic spines [Kramer and Schulz-Schaeffer, 2007,Zaja-Milatovic, et al.,2006].

Occipital hypometabolism in DLB is associated with visual hallucinations [Imamura, et al., 1999,Perneczky, et al.,2008]. It was not possible to assess whether visual hallucinations were associated with occipital hypometabolism in our cohort because only two of the DLB patients did not have visual hallucinations. On the other hand, we found greater occipital hypometabolism in DLB patients with more frequent visual hallucinations, longer duration of pRBD and fluctuations. Collectively, these data indicate that there is a relationship between the regional hypometabolism on FDG PET and clinical features of DLB further supporting our finding that the occipital lobe and posterior parietotemporal hypometabolism is associated with LRP in patients with DLB. We note that one of the autopsy-confirmed AD patients (Case 1) with advanced AD pathology and no LB pathology also had occipital hypometabolism most likely due to the severe AD pathology. Occipital metabolism declines in advanced AD [Ishii, etal.,1997], and is associated with atypical AD [Aharon-Peretz, et al., 1999] with posterior atrophy syndrome [Hof, et al.,1997,Tang-Wai, et al.,2004] therefore occipital hypometabolism is not a specific marker for DLB, and can occasionally be associated with AD. In some AD patients with posterior cortical atrophy, there is relative sparing of the hippocampus [Tang-Wai, et al.,2004] making the differential diagnosis in these rare cases even more difficult. In most cases however it may be possible to distinguish atypical AD from DLB by combining imaging markers associated with AD pathology such as high PiB retention, demonstrating the potential value of multimodality imaging in distinguishing DLB and AD in most cases.

## Value of multimodality imaging for distinguishing patients with AD and DLB

When each imaging marker was considered separately, we found overlap between the AD and DLB groups among the imaging markers that best distinguished patients AD and DLB. Each imaging marker contributed significantly to the logistic regression model and the accuracy for distinguishing patients with AD and DLB improved to 98% when all three imaging markers were considered (Figure 6). Discrimination of the autopsy-confirmed DLB cases were highly accurate when at least two of the imaging markers were considered. Among the two AD cases, Case 1 had occipital hypometabolism likely due to severe AD pathology and Case 2 had low PiB retention in agreement with the pathological diagnosis of

low likelihood of AD but had moderate hippocampal atrophy possibly due to both mild AD pathology and argyrophilic grain disease in the hippocampus. Distinguishing these cases from patients with DLB was possible only with multimodality imaging. Two of the DLB cases (Case 3 and Case 4) had borderline PiB retention and mild hippocampal atrophy likely due to the presence of mild AD pathology but Case 3 had significantly low occipital FDG uptake that distinguished this case from patients with AD. In Case 5 with a low likelihood of AD and high likelihood of DLB, we found high PiB retention that was largely attributed to the frequent diffuse plaques. All autopsy confirmed DLB patients were distinguished from AD using multimodality imaging however a single imaging finding was typically insufficient for distinguishing cases with DLB from AD.

The clinical diagnosis of patients in the current study was made with standard clinical criteria using the core and suggestive features for probable DLB and probable AD [McKeith, et al.,2005,McKhann, et al.,1984]. Imaging the impaired nigrostriatal dopamine innervation with PET and SPECT is important for differential diagnosis of Lewy body disoders [Bohnen and Frey,2007,Ceravolo, et al.,2004,Gilman, et al.,2004,Koeppe, et al., 2005,McKeith, et al.,2007,O'Brien, et al.,2004,O'Brien, et al.,2009,Seibyl, et al., 1996,Walker, et al.,2007] and offers complementary information to FDG PET for differentiation of AD and DLB [Koeppe, et al.,2005].Impaired nigrostriatal dopamine innervation is now considered a suggestive feature for the clinical diagnosis of DLB [McKeith, et al.,2005]. While we did not benefit from the additional information dopamine transporter imaging would provide for the clinical diagnosis of DLB in our cohort, the imaging markers we evaluated were not used for the clinical diagnosis of DLB patients.

The strength of our study is multimodality imaging that was performed in all participants within a short time interval. Imaging findings in the five autopsy-confirmed cases of this cohort further verify our observations on the complementary nature of multimodality imaging in characterizing the underlying pathology in DLB. We note that each imaging abnormality is typically associated with a feature of AD pathology or LRP but they are not highly specific. Furthermore, AD pathology is common in patients with DLB and may be associated with the borderline imaging features of AD in patients with DLB. The moderately increased PiB retention in DLB may be associated with either diffuse plaques that are common in DLB or moderate neuritic plaques associated with AD pathology [Burack, et al., 2010,Kantarci, et al.,2010] Hippocampal atrophy is a sensitive but not a specific marker for the neurofibrillary pathology of AD [Burton, et al.,2009,Kantarci, et al.,2011] and is complementary to the PET imaging markers for the differential diagnosis of DLB and AD. We demonstrate the value of multimodality imaging in characterizing patients with DLB in whom the pathophysiological mechanisms of dementia are complex.

## Acknowledgments

This work was supported by the National Institutes of Health: K23-AG030935 and P50-AG16574/P1 to KK, R01-AG015866 to TJF, R01-AG11378 to CRJ, P50-AG16574 and U01-AG06786 to RCP; Mangurian Foundation to BFB, TJF and DWD, and the Robert H. and Clarice Smith and Abigail Van Buren Alzheimer's Disease Research Program.

## References

AASM. International Classification of Sleep Disorders—2: Diagnostic and Coding Manual. Chicago: American Academy of Sleep Medicine; 2005.

Aharon-Peretz J, Israel O, Goldsher D, Peretz A. Posterior cortical atrophy variants of Alzheimer's disease. Dement Geriatr Cogn Disord. 1999; 10(6):483–487. [PubMed: 10559564]

Albin RL, Minoshima S, D'Amato CJ, Frey KA, Kuhl DA, Sima AA. Fluoro-deoxyglucose positron emission tomography in diffuse Lewy body disease. Neurology. 1996; 47(2):462–466. [PubMed: 8757021]

Ashburner J, Friston KJ. Unified segmentation. Neuroimage. 2005; 26(3):839–851. [PubMed: 15955494]

Barber R, Gholkar A, Scheltens P, Ballard C, McKeith L, O'Brien J. Medial temporal lobe atrophy on MRI in dementia with Lewy bodies. Neurology. 1999; 52:1153–1158. [PubMed: 10214736]

Barker WW, Luis CA, Kashuba A, Luis M, Harwood DG, Loewenstein D, Waters C, Jimison P, Shepherd E, Sevush S, Graff-Radford N, Newland D, Todd M, Miller B, Gold M, Heilman K, Doty L, Goodman I, Robinson B, Pearl G, Dickson D, Duara R. Relative frequencies of Alzheimer disease, Lewy body, vascular and frontotemporal dementia, and hippocampal sclerosis in the State of Florida Brain Bank. Alzheimer Dis Assoc Disord. 2002; 16(4):203–212. [PubMed: 12468894]

Barkhof F, Polvikoski TM, van Straaten EC, Kalaria RN, Sulkava R, Aronen HJ, Niinisto L, Rastas S, Oinas M, Scheltens P, Erkinjuntti T. The significance of medial temporal lobe atrophy: a postmortem MRI study in the very old. Neurology. 2007; 69(15):1521–1527. [PubMed: 17923614]

Bobinski M, Wegiel J, Tarnawski M, Reisberg B, de Leon MJ, Miller DC, Wisniewski HM. Relationships between regional neuronal loss and neurofibrillary changes in the hippocampal formation and duration and severity of Alzheimer disease. Journal of Neuropathology & Experimental Neurology. 1997; 56(4):414–420. [PubMed: 9100672]

Bohnen NI, Frey KA. Imaging of cholinergic and monoaminergic neurochemical changes in neurodegenerative disorders. Mol Imaging Biol. 2007; 9(4):243–257. [PubMed: 17318670]

Braak H, Braak E. Neuropathological stageing of Alzheimer-related changes. Acta Neuropathol. 1991; 82(4):239–259. [PubMed: 1759558]

Burack MA, Hartlein J, Flores HP, Taylor-Reinwald L, Perlmutter JS, Cairns NJ. In vivo amyloid imaging in autopsy-confirmed Parkinson disease with dementia. Neurology. 2010; 74(1):77–84. [PubMed: 20038776]

Burton EJ, Barber R, Mukaetova-Ladinska EB, Robson J, Perry RH, Jaros E, Kalaria RN, O'Brien JT. Medial temporal lobe atrophy on MRI differentiates Alzheimer's disease from dementia with Lewy bodies and vascular cognitive impairment: a prospective study with pathological verification of diagnosis. Brain. 2009; 132(Pt 1):195–203. [PubMed: 19022858]

Burton EJ, Karas G, Paling SM, Barber R, Williams ED, Ballard CG, McKeith IG, Scheltens P, Barkhof F, O'Brien JT. Patterns of cerebral atrophy in dementia with Lewy bodies using voxel-based morphometry. Neuroimage. 2002; 17(2):618–630. [PubMed: 12377138]

Burton EJ, Mukaetova-Ladinska EB, Perry RH, Jaros E, Barber R, O'Brien JT. Neuropathological correlates of volumetric MRI in autopsy-confirmed Lewy body dementia. Neurobiol Aging. 2011

Ceravolo R, Volterrani D, Gambaccini G, Bernardini S, Rossi C, Logi C, Tognoni G, Manca G, Mariani G, Bonuccelli U, Murri L. Presynaptic nigro-striatal function in a group of Alzheimer's disease patients with parkinsonism: evidence from a dopamine transporter imaging study. J Neural Transm. 2004; 111(8):1065–1073. [PubMed: 15254794]

Csernansky JG, Hamstra J, Wang L, McKeel D, Price JL, Gado M, Morris JC. Correlations between antemortem hippocampal volume and postmortem neuropathology in AD subjects. Alzheimer Dis Assoc Disord. 2004; 18(4):190–195. [PubMed: 15592129]

Dickson DW. Dementia with Lewy bodies: neuropathology. J Geriatr Psychiatry Neurol. 2002; 15(4): 210–216. [PubMed: 12489917]

Dickson DW, Crystal HA, Bevona C, Honer W, Vincent I, Davies P. Correlations of synaptic and pathological markers with cognition of the elderly. Neurobiol Aging. 1995; 16(3):285–98. discussion 98–304. [PubMed: 7566338]

Dickson DW, Ruan D, Crystal H, Mark MH, Davies P, Kress Y, Yen SH. Hippocampal degeneration differentiates diffuse Lewy body disease (DLBD) from Alzheimer's disease: light and electron microscopic immunocytochemistry of CA2–3 neurites specific to DLBD. Neurology. 1991; 41(9): 1402–1409. [PubMed: 1653914]

Edison P, Rowe CC, Rinne JO, Ng S, Ahmed I, Kemppainen N, Villemagne VL, O'Keefe G, Nagren K, Chaudhury KR, Masters CL, Brooks DJ. Amyloid load in Parkinson's disease dementia and

Lewy body dementia measured with [11C]PIB positron emission tomography. J Neurol Neurosurg Psychiatry. 2008; 79(12):1331–1338. [PubMed: 18653550]

Ferman TJ, Smith GE, Boeve BF, Ivnik RJ, Petersen RC, Knopman D, Graff-Radford N, Parisi J, Dickson DW. DLB fluctuations: specific features that reliably differentiate DLB from AD and normal aging. Neurology. 2004; 62(2):181–187. [PubMed: 14745051]

Firbank MJ, Blamire AM, Teodorczuk A, Teper E, Burton EJ, Mitra D, O'Brien JT. High resolution imaging of the medial temporal lobe in Alzheimer's disease and dementia with Lewy bodies. J Alzheimers Dis. 2010; 21(4):1129–1140. [PubMed: 21504120]

Fodero-Tavoletti MT, Smith DP, McLean CA, Adlard PA, Barnham KJ, Foster LE, Leone L, Perez K, Cortes M, Culvenor JG, Li QX, Laughton KM, Rowe CC, Masters CL, Cappai R, Villemagne VL. In vitro characterization of Pittsburgh compound-B binding to Lewy bodies. J Neurosci. 2007; 27(39):10365–10371. [PubMed: 17898208]

Foster ER, Campbell MC, Burack MA, Hartlein J, Flores HP, Cairns NJ, Hershey T, Perlmutter JS. Amyloid imaging of Lewy body-associated disorders. Mov Disord. 2010; 25(15):2516–2523. [PubMed: 20922808]

Fujishiro H, Ferman TJ, Boeve BF, Smith GE, Graff-Radford NR, Uitti RJ, Wszolek ZK, Knopman DS, Petersen RC, Parisi JE, Dickson DW. Validation of the neuropathologic criteria of the third consortium for dementia with Lewy bodies for prospectively diagnosed cases. J Neuropathol Exp Neurol. 2008; 67(7):649–656. [PubMed: 18596548]

Fujishiro H, Iseki E, Higashi S, Kasanuki K, Murayama N, Togo T, Katsuse O, Uchikado H, Aoki N, Kosaka K, Arai H, Sato K. Distribution of cerebral amyloid deposition and its relevance to clinical phenotype in Lewy body dementia. Neurosci Lett. 2010; 486(1):19–23. [PubMed: 20851165]

Galasko D, Hansen LA, Katzman R, Wiederholt W, Masliah E, Terry R, Hill LR, Lessin P, Thal LJ. Clinical-neuropathological correlations in Alzheimer's disease and related dementias. Arch Neurol. 1994; 51(9):888–895. [PubMed: 8080388]

Giannakopoulos P, Hof PR, Mottier S, Michel JP, Bouras C. Neuropathological changes in the cerebral cortex of 1258 cases from a geriatric hospital: retrospective clinicopathological evaluation of a 10-year autopsy population. Acta Neuropathol. 1994; 87(5):456–468. [PubMed: 8059598]

Gilman S, Koeppe RA, Little R, An H, Junck L, Giordani B, Persad C, Heumann M, Wernette K. Striatal monoamine terminals in Lewy body dementia and Alzheimer's disease. Ann Neurol. 2004; 55(6):774–780. [PubMed: 15174011]

Gomez-Isla T, Hollister R, West H, Mui S, Growdon JH, Petersen RC, Parisi JE, Hyman BT. Neuronal loss correlates with but exceeds neurofibrillary tangles in Alzheimer's disease. Annals of Neurology. 1997; 41(1):17–24. [PubMed: 9005861]

Gomez-Tortosa E, Newell K, Irizarry MC, Albert M, Growdon JH, Hyman BT. Clinical and quantitative pathologic correlates of dementia with Lewy bodies. Neurology. 1999; 53(6):1284–1291. [PubMed: 10522886]

Gomperts SN, Rentz DM, Moran E, Becker JA, Locascio JJ, Klunk WE, Mathis CA, Elmaleh DR, Shoup T, Fischman AJ, Hyman BT, Growdon JH, Johnson KA. Imaging amyloid deposition in Lewy body diseases. Neurology. 2008; 71(12):903–910. [PubMed: 18794492]

Gosche KM, Mortimer JA, Smith CD, Markesbery WR, Snowdon DA. Hippocampal volume as an index of Alzheimer neuropathology: findings from the Nun Study. Neurology. 2002; 58(10):1476–1482. [PubMed: 12034782]

Grober E, Dickson D, Sliwinski MJ, Buschke H, Katz M, Crystal H, Lipton RB. Memory and mental status correlates of modified Braak staging. Neurobiology of Aging. 1999; 20(6):573–579. [PubMed: 10674422]

Guillozed AL, Weintraub S, Mash DC, Mesulam MM. Neurofibrillary tangles, amyloid, and memory in aging and mild cognitive impairment. Archives of Neurology. 2003; 60(5):729–736. [PubMed: 12756137]

Hansen L, Salmon D, Galasko D, Masliah E, Katzman R, DeTeresa R, Thal L, Pay MM, Hofstetter R, Klauber M, et al. The Lewy body variant of Alzheimer's disease: a clinical and pathologic entity. Neurology. 1990; 40(1):1–8. [PubMed: 2153271]

Harrell, FEJ., editor. Regression modeling strategies. New York: Springer; 2001.

Higuchi M, Tashiro M, Arai H, Okamura N, Hara S, Higuchi S, Itoh M, Shin RW, Trojanowski JQ, Sasaki H. Glucose hypometabolism and neuropathological correlates in brains of dementia with Lewy bodies. Exp Neurol. 2000; 162(2):247–256. [PubMed: 10739631]

Hof PR, Vogt BA, Bouras C, Morrison JH. Atypical form of Alzheimer's disease with prominent posterior cortical atrophy: a review of lesion distribution and circuit disconnection in cortical visual pathways. Vision Res. 24; 37:3609–3625. [PubMed: 9425534]

Hyman BT, Trojanowski JQ. Consensus recommendations for the postmortem diagnosis of Alzheimer disease from the National Institute on Aging and the Reagan Institute Working Group on diagnostic criteria for the neuropathological assessment of Alzheimer disease. J Neuropathol Exp Neurol. 1997; 56(10):1095–1097. [PubMed: 9329452]

Ikonomovic MD, Klunk WE, Abrahamson EE, Mathis CA, Price JC, Tsopelas ND, Lopresti BJ, Ziolko S, Bi W, Paljug WR, Debnath ML, Hope CE, Isanski BA, Hamilton RL, Dekosky ST. Post-mortem correlates of in vivo PiB-PET amyloid imaging in a typical case of Alzheimer's disease. Brain. 2008

Imamura T, Ishii K, Hirono N, Hashimoto M, Tanimukai S, Kazuai H, Hanihara T, Sasaki M, Mori E. Visual hallucinations and regional cerebral metabolism in dementia with Lewy bodies (DLB). Neuroreport. 1999; 10(9):1903–1907. [PubMed: 10501530]

Imamura T, Ishii K, Sasaki M, Kitagaki H, Yamaji S, Hirono N, Shimomura T, Hashimoto M, Tanimukai S, Kazui H, Mori E. Regional cerebral glucose metabolism in dementia with Lewy bodies and Alzheimer's disease: a comparative study using positron emission tomography. Neurosci Lett. 1997; 235(1–2):49–52. [PubMed: 9389593]

Ishii K, Imamura T, Sasaki M, Yamaji S, Sakamoto S, Kitagaki H, Hashimoto M, Hirono N, Shimomura T, Mori E. Regional cerebral glucose metabolism in dementia with Lewy bodies and Alzheimer's disease. Neurology. 1998; 51(1):125–130. [PubMed: 9674790]

Ishii K, Sasaki M, Kitagaki H, Yamaji S, Sakamoto S, Matsuda K, Mori E. Reduction of cerebellar glucose metabolism in advanced Alzheimer's disease. J Nucl Med. 1997; 38(6):925–928. [PubMed: 9189143]

Jack CR Jr, Dickson DW, Parisi JE, Xu YC, Cha RH, O'Brien PC, Edland SD, Smith GE, Boeve BF, Tangalos EG, Kokmen E, Petersen RC. Antemortem MRI findings correlate with hippocampal neuropathology in typical aging and dementia. Neurology. 2002; 58(5):750–757. [PubMed: 11889239]

Jack CR Jr, Lowe VJ, Senjem ML, Weigand SD, Kemp BJ, Shiung MM, Knopman DS, Boeve BF, Klunk WE, Mathis CA, Petersen RC. 11C PiB and structural MRI provide complementary information in imaging of Alzheimer's disease and amnestic mild cognitive impairment. Brain. 2008; 131(Pt 3):665–680. [PubMed: 18263627]

Jack CRJ, Lowe VJ, Senjem ML, Weigand SD, Shiung MM, Kemp BJ, Knopman DS, et al. 11C PiB and Structural MRI porvide complementary information in imaging of AD and amnestic MCI. 2007 In Press Brain.

Jagust WJ, Zheng L, Harvey DJ, Mack WJ, Vinters HV, Weiner MW, Ellis WG, Zarow C, Mungas D, Reed BR, Kramer JH, Schuff N, DeCarli C, Chui HC. Neuropathological basis of magnetic resonance images in aging and dementia. Ann Neurol. 2008; 63(1):72–80. [PubMed: 18157909]

Joachim CL, Morris JH, Selkoe DJ. Clinically diagnosed Alzheimer's disease: autopsy results in 150 cases. Ann Neurol. 1988; 24(1):50–56. [PubMed: 3415200]

Kalaitzakis ME, Walls AJ, Pearce RK, Gentleman SM. Striatal Abeta peptide deposition mirrors dementia and differentiates DLB and PDD from other Parkinsonian syndromes. Neurobiol Dis. 2011; 41(2):377–384. [PubMed: 20951207]

Kantarci K, Dickson DW, Vemuri P, Ferman TJ, Boeve BF, Smith GE, Senjem ML, Parisi JE, Weigand SD, Murray MM, Knopman DS, Petersen RC, Jack CR. Antemortem Hippocampal Atrophy Predicts Presence of Alzheimer's Disease Pathology in Pathologically Proven Lewy Body Disease. Neurology. 2011; 76 Suppl.4(9):176.

Kantarci K, Senjem ML, Lowe VJ, Wiste HJ, Weigand SD, Kemp BJ, Frank AR, Shiung MM, Boeve BF, Knopman DS, Petersen RC, Jack CR Jr. Effects of age on the glucose metabolic changes in mild cognitive impairment impairment. AJNR Am J Neuroradiol. 2010; 31(7):1247–1253. [PubMed: 20299441]

Kantarci K, Yang C, Schneider JA, Senjem ML, Reyes DA, Lowe VJ, Barnes LL, Aggarwal NT, Bennett DA, Smith GE, Petersen RC, Jack CR Jr, Boeve BF. Ante mortem amyloid imaging and beta-amyloid pathology in a case with dementia with Lewy bodies. Neurobiol Aging (epub ahead of print). 2010

Koeppe RA, Gilman S, Joshi A, Liu S, Little R, Junck L, Heumann M, Frey KA, Albin RL. 11C–DTBZ and 18F–FDG PET measures in differentiating dementias. J Nucl Med. 2005; 46(6):936–944. [PubMed: 15937303]

Kramer ML, Schulz-Schaeffer WJ. Presynaptic alpha-synuclein aggregates, not Lewy bodies, cause neurodegeneration in dementia with Lewy bodies. J Neurosci. 2007; 27(6):1405–1410. [PubMed: 17287515]

Lim SM, Katsifis A, Villemagne VL, Best R, Jones G, Saling M, Bradshaw J, Merory J, Woodward M, Hopwood M, Rowe CC. The 18F–FDG PET cingulate island sign and comparison to 123I–beta-CIT SPECT for diagnosis of dementia with Lewy bodies. J Nucl Med. 2009; 50(10):1638–1645. [PubMed: 19759102]

Lippa C, Johnson R, Smith T. The medial temporal lobe in dementia with Lewy bodies: a comparative study with Alzheimer's disease. Ann Neurol. 1998; 43:102–106. [PubMed: 9450774]

Lockhart A, Lamb JR, Osredkar T, Sue LI, Joyce JN, Ye L, Libri V, Leppert D, Beach TG. PIB is a non-specific imaging marker of amyloid-beta (Abeta) peptide-related cerebral amyloidosis. Brain. 2007; 130(Pt 10):2607–2615. [PubMed: 17698496]

Lowe VJ, Kemp BJ, Jack CR Jr, Senjem M, Weigand S, Shiung M, Smith G, Knopman D, Boeve B, Mullan B, Petersen RC. Comparison of 18F–FDG and PiB PET in cognitive impairment. J Nucl Med. 2009; 50(6):878–886. [PubMed: 19443597]

Luis CA, Barker WW, Gajaraj K, Harwood D, Petersen R, Kashuba A, Waters C, Jimison P, Pearl G, Petito C, Dickson D, Duara R. Sensitivity and specificity of three clinical criteria for dementia with Lewy bodies in an autopsy-verified sample. Int J Geriatr Psychiatry. 1999; 14(7):526–533. [PubMed: 10440972]

Maetzler W, Liepelt I, Reimold M, Reischl G, Solbach C, Becker C, Schulte C, Leyhe T, Keller S, Melms A, Gasser T, Berg D. Cortical PIB binding in Lewy body disease is associated with Alzheimer-like characteristics. Neurobiol Dis. 2009; 34(1):107–112. [PubMed: 19162186]

McKeith I, O'Brien J, Walker Z, Tatsch K, Booij J, Darcourt J, Padovani A, Giubbini R, Bonuccelli U, Volterrani D, Holmes C, Kemp P, Tabet N, Meyer I, Reininger C. Sensitivity and specificity of dopamine transporter imaging with 123I–FP-CIT SPECT in dementia with Lewy bodies: a phase III, multicentre study. Lancet Neurol. 2007; 6(4):305–313. [PubMed: 17362834]

McKeith IG, Ballard CG, Perry RH, Ince PG, O'Brien JT, Neill D, Lowery K, Jaros E, Barber R, Thompson P, Swann A, Fairbairn AF, Perry EK. Prospective validation of consensus criteria for the diagnosis of dementia with Lewy bodies. Neurology. 2000; 54(5):1050–1058. [PubMed: 10720273]

McKeith IG, Dickson DW, Lowe J, Emre M, O'Brien JT, Feldman H, Cummings J, Duda JE, Lippa C, Perry EK, Aarsland D, Arai H, Ballard CG, Boeve B, Burn DJ, Costa D, Del Ser T, Dubois B, Galasko D, Gauthier S, Goetz CG, Gomez-Tortosa E, Halliday G, Hansen LA, Hardy J, Iwatsubo T, Kalaria RN, Kaufer D, Kenny RA, Korczyn A, Kosaka K, Lee VM, Lees A, Litvan I, Londos E, Lopez OL, Minoshima S, Mizuno Y, Molina JA, Mukaetova-Ladinska EB, Pasquier F, Perry RH, Schulz JB, Trojanowski JQ, Yamada M. Diagnosis and management of dementia with Lewy bodies: third report of the DLB Consortium. Neurology. 2005; 65(12):1863–1872. [PubMed: 16237129]

McKhann G, Drachman D, Folstein M, Katzman R, Price D, Stadlan EM. Clinical diagnosis of Alzheimer's disease: report of the NINCDS-ADRDA Work Group under the auspices of Department of Health and Human Services Task Force on Alzheimer's Disease. Neurology. 1984; 34(7):939–944. [PubMed: 6610841]

Meltzer CC, Kinahan PE, Greer PJ, Nichols TE, Comtat C, Cantwell MN, Lin MP, Price JC. Comparative evaluation of MR-based partial-volume correction schemes for PET. J Nucl Med. 1999; 40(12):2053–2065. [PubMed: 10616886]

Merdes AR, Hansen LA, Jeste DV, Galasko D, Hofstetter CR, Ho GJ, Thal LJ, Corey-Bloom J. Influence of Alzheimer pathology on clinical diagnostic accuracy in dementia with Lewy bodies. Neurology. 2003; 60(10):1586–1590. [PubMed: 12771246]

Minoshima S, Foster NL, Sima AA, Frey KA, Albin RL, Kuhl DE. Alzheimer's disease versus dementia with Lewy bodies: cerebral metabolic distinction with autopsy confirmation. Ann Neurol. 2001; 50(3):358–365. [PubMed: 11558792]

Mirra SS, Heyman A, McKeel D, Sumi SM, Crain BJ, Brownlee LM, Vogel FS, Hughes JP, van Belle G, Berg L. The Consortium to Establish a Registry for Alzheimer's Disease (CERAD). Part II. Standardization of the neuropathologic assessment of Alzheimer's disease. Neurology. 1991; 41(4):479–486. [PubMed: 2011243]

Mori T, Ikeda M, Fukuhara R, Nestor PJ, Tanabe H. Correlation of visual hallucinations with occipital rCBF changes by donepezil in DLB. Neurology. 2006; 66(6):935–937. [PubMed: 16567718]

Mosconi L, Tsui WH, Herholz K, Pupi A, Drzezga A, Lucignani G, Reiman EM, Holthoff V, Kalbe E, Sorbi S, Diehl-Schmid J, Perneczky R, Clerici F, Caselli R, Beuthien-Baumann B, Kurz A, Minoshima S, de Leon MJ. Multicenter standardized 18F–FDG PET diagnosis of mild cognitive impairment, Alzheimer's disease, and other dementias. J Nucl Med. 2008; 49(3):390–398. [PubMed: 18287270]

Nagy Z, Esiri MM, Jobst KA, Morris JH, King EM, McDonald B, Litchfield S, Smith A, Barnetson L, Smith AD. Relative roles of plaques and tangles in the dementia of Alzheimer's disease: correlations using three sets of neuropathological criteria. Dementia. 1995; 6(1):21–31. [PubMed: 7728216]

O'Brien JT, Colloby S, Fenwick J, Williams ED, Firbank M, Burn D, Aarsland D, McKeith IG. Dopamine transporter loss visualized with FP-CIT SPECT in the differential diagnosis of dementia with Lewy bodies. Arch Neurol. 2004; 61(6):919–925. [PubMed: 15210531]

O'Brien JT, McKeith IG, Walker Z, Tatsch K, Booij J, Darcourt J, Marquardt M, Reininger C. Diagnostic accuracy of 123I–FP-CIT SPECT in possible dementia with Lewy bodies. Br J Psychiatry. 2009; 194(1):34–39. [PubMed: 19118323]

Perneczky R, Drzezga A, Boecker H, Forstl H, Kurz A, Haussermann P. Cerebral metabolic dysfunction in patients with dementia with Lewy bodies and visual hallucinations. Dement Geriatr Cogn Disord. 2008; 25(6):531–538. [PubMed: 18477846]

Quigley H, Colloby SJ, O'Brien JT. PET imaging of brain amyloid in dementia: a review. Int J Geriatr Psychiatry [Epub ahead of print]. 2010

Roberts RO, Geda YE, Knopman DS, Cha RH, Pankratz VS, Boeve BF, Ivnik RJ, Tangalos EG, Petersen RC, Rocca WA. The Mayo Clinic Study of Aging: design and sampling, participation, baseline measures and sample characteristics. Neuroepidemiology. 2008; 30(1):58–69. [PubMed: 18259084]

Rocher AB, Chapon F, Blaizot X, Baron JC, Chavoix C. Resting-state brain glucose utilization as measured by PET is directly related to regional synaptophysin levels: a study in baboons. Neuroimage. 2003; 20(3):1894–1898. [PubMed: 14642499]

Rowe CC, Ng S, Ackermann U, Gong SJ, Pike K, Savage G, Cowie TF, Dickinson KL, Maruff P, Darby D, Smith C, Woodward M, Merory J, Tochon-Danguy H, O'Keefe G, Klunk WE, Mathis CA, Price JC, Masters CL, Villemagne VL. Imaging beta-amyloid burden in aging and dementia. Neurology. 2007; 68(20):1718–1725. [PubMed: 17502554]

Sabattoli F, Boccardi M, Galluzzi S, Treves A, Thompson PM, Frisoni GB. Hippocampal shape differences in dementia with Lewy bodies. Neuroimage. 2008; 41(3):699–705. [PubMed: 18467130]

Satoh M, Ishikawa H, Meguro K, Kasuya M, Ishii H, Yamaguchi S. Improved visual hallucination by donepezil and occipital glucose metabolism in dementia with Lewy bodies: the Osaki-Tajiri project. Eur Neurol. 2010; 64(6):337–344. [PubMed: 21071950]

Schneider JA, Arvanitakis Z, Bang W, Bennett DA. Mixed brain pathologies account for most dementia cases in community-dwelling older persons. Neurology. 2007; 69(24):2197–2204. [PubMed: 17568013]

Seibyl JP, Laruelle M, van Dyck CH, Wallace E, Baldwin RM, Zoghbi S, Zea-Ponce Y, Neumeyer JL, Charney DS, Hoffer PB, Innis RB. Reproducibility of iodine-123-beta-CIT SPECT brain measurement of dopamine transporters. J Nucl Med. 1996; 37(2):222–228. [PubMed: 8667048]

Shimada H, Hirano S, Shinotoh H, Aotsuka A, Sato K, Tanaka N, Ota T, Asahina M, Fukushi K, Kuwabara S, Hattori T, Suhara T, Irie T. Mapping of brain acetylcholinesterase alterations in Lewy body disease by PET. Neurology. 2009; 73(4):273–278. [PubMed: 19474411]

Silbert LC, Quinn JF, Moore MM, Corbridge E, Ball MJ, Murdoch G, Sexton G, Kaye JA. Changes in premorbid brain volume predict Alzheimer's disease pathology. Neurology. 2003; 61(4):487–492. [PubMed: 12939422]

Sojkova J, Driscoll I, Iacono D, Zhou Y, Codispoti KE, Kraut MA, Ferrucci L, Pletnikova O, Mathis CA, Klunk WE, O'Brien RJ, Wong DF, Troncoso JC, Resnick SM. In Vivo Fibrillar {beta}-Amyloid Detected Using [11C]PiB Positron Emission Tomography and Neuropathologic Assessment in Older Adults. Arch Neurol. 2011; 68(2):232–240. [PubMed: 21320990]

Tam CW, Burton EJ, McKeith IG, Burn DJ, O'Brien JT. Temporal lobe atrophy on MRI in Parkinson disease with dementia: a comparison with Alzheimer disease and dementia with Lewy bodies. Neurology. 2005; 64(5):861–865. [PubMed: 15753423]

Tang-Wai DF, Graff-Radford NR, Boeve BF, Dickson DW, Parisi JE, Crook R, Caselli RJ, Knopman DS, Petersen RC. Clinical, genetic, and neuropathologic characteristics of posterior cortical atrophy. Neurology. 2004; 63(7):1168–1174. [PubMed: 15477533]

Teune LK, Bartels AL, de Jong BM, Willemsen AT, Eshuis SA, de Vries JJ, van Oostrom JC, Leenders KL. Typical cerebral metabolic patterns in neurodegenerative brain diseases. Mov Disord. 2010; 25(14):2395–2404. [PubMed: 20669302]

The National Institute on Aging aRIwGoDCftNAoAsD. Consensus recommendations for the postmortem diagnosis of Alzheimer's Disease. Neurobiology of Aging. 1997; (18):S1–S2. [PubMed: 9330978]

Tzourio-Mazoyer N, Landeau B, Papathanassiou D, Crivello F, Etard O, Delcroix N, Mazoyer B, Joliot M. Automated anatomical labeling of activations in SPM using a macroscopic anatomical parcellation of the MNI MRI single-subject brain. Neuroimage. 2002; 15(1):273–289. [PubMed: 11771995]

Vemuri P, Gunter JL, Senjem ML, Whitwell JL, Kantarci K, Knopman DS, Boeve BF, Petersen RC, Jack CR Jr. Alzheimer's disease diagnosis in individual subjects using structural MR images: validation studies. Neuroimage. 2008; 39(3):1186–1197. [PubMed: 18054253]

Vemuri P, Simon G, Kantarci K, Whitwell JL, Senjem ML, Przybelski SA, Gunter JL, Josephs KA, Knopman DS, Boeve BF, Ferman TJ, Dickson DW, Parisi JE, Petersen RC, Jack CR Jr. Antemortem differential diagnosis of dementia pathology using structural MRI: Differential-STAND. Neuroimage. 2010; 55(2):522–531. [PubMed: 21195775]

Vemuri P, Whitwell JL, Kantarci K, Josephs KA, Parisi JE, Shiung MS, Knopman DS, Boeve BF, Petersen RC, Dickson DW, Jack CR Jr. Antemortem MRI based Structural Abnormality iNDex (STAND)-scores correlate with postmortem Braak neurofibrillary tangle stage. Neuroimage. 2008; 42(2):559–567. [PubMed: 18572417]

Verghese J, Crystal HA, Dickson DW, Lipton RB. Validity of clinical criteria for the diagnosis of dementia with Lewy bodies. Neurology. 1999; 53(9):1974–1982. [PubMed: 10599768]

Walker Z, Jaros E, Walker RW, Lee L, Costa DC, Livingston G, Ince PG, Perry R, McKeith I, Katona CL. Dementia with Lewy bodies: a comparison of clinical diagnosis, FP- CIT single photon emission computed tomography imaging and autopsy. J Neurol Neurosurg Psychiatry. 2007; 78(11):1176–1181. [PubMed: 17353255]

Whitwell JL, Josephs KA, Murray ME, Kantarci K, Przybelski SA, Weigand SD, Vemuri P, Senjem ML, Parisi JE, Knopman DS, Boeve BF, Petersen RC, Dickson DW, Jack CR Jr. MRI correlates of neurofibrillary tangle pathology at autopsy: a voxel-based morphometry study. Neurology. 2008; 71(10):743–749. [PubMed: 18765650]

Whitwell JL, Weigand SD, Shiung MM, Boeve BF, Ferman TJ, Smith GE, Knopman DS, Petersen RC, Benarroch EE, Josephs KA, Jack CR Jr. Focal atrophy in dementia with Lewy bodies on MRI: a distinct pattern from Alzheimer's disease. Brain. 2007; 130(Pt 3):708–719. [PubMed: 17267521]

Ye L, Velasco A, Fraser G, Beach TG, Sue L, Osredkar T, Libri V, Spillantini MG, Goedert M, Lockhart A. In vitro high affinity alpha-synuclein binding sites for the amyloid imaging agent PIB are not matched by binding to Lewy bodies in postmortem human brain. J Neurochem. 2008

Zaccai J, McCracken C, Brayne C. A systematic review of prevalence and incidence studies of dementia with Lewy bodies. Age Ageing. 2005; 34(6):561–566. [PubMed: 16267179]

Zaja-Milatovic S, Keene CD, Montine KS, Leverenz JB, Tsuang D, Montine TJ. Selective dendritic degeneration of medium spiny neurons in dementia with Lewy bodies. Neurology. 2006; 66(10): 1591–1593. [PubMed: 16717229]

Zarow C, Vinters HV, Ellis WG, Weiner MW, Mungas D, White L, Chui HC. Correlates of hippocampal neuron number in Alzheimer's disease and ischemic vascular dementia. Ann Neurol. 2005; 57(6):896–903. [PubMed: 15929035]

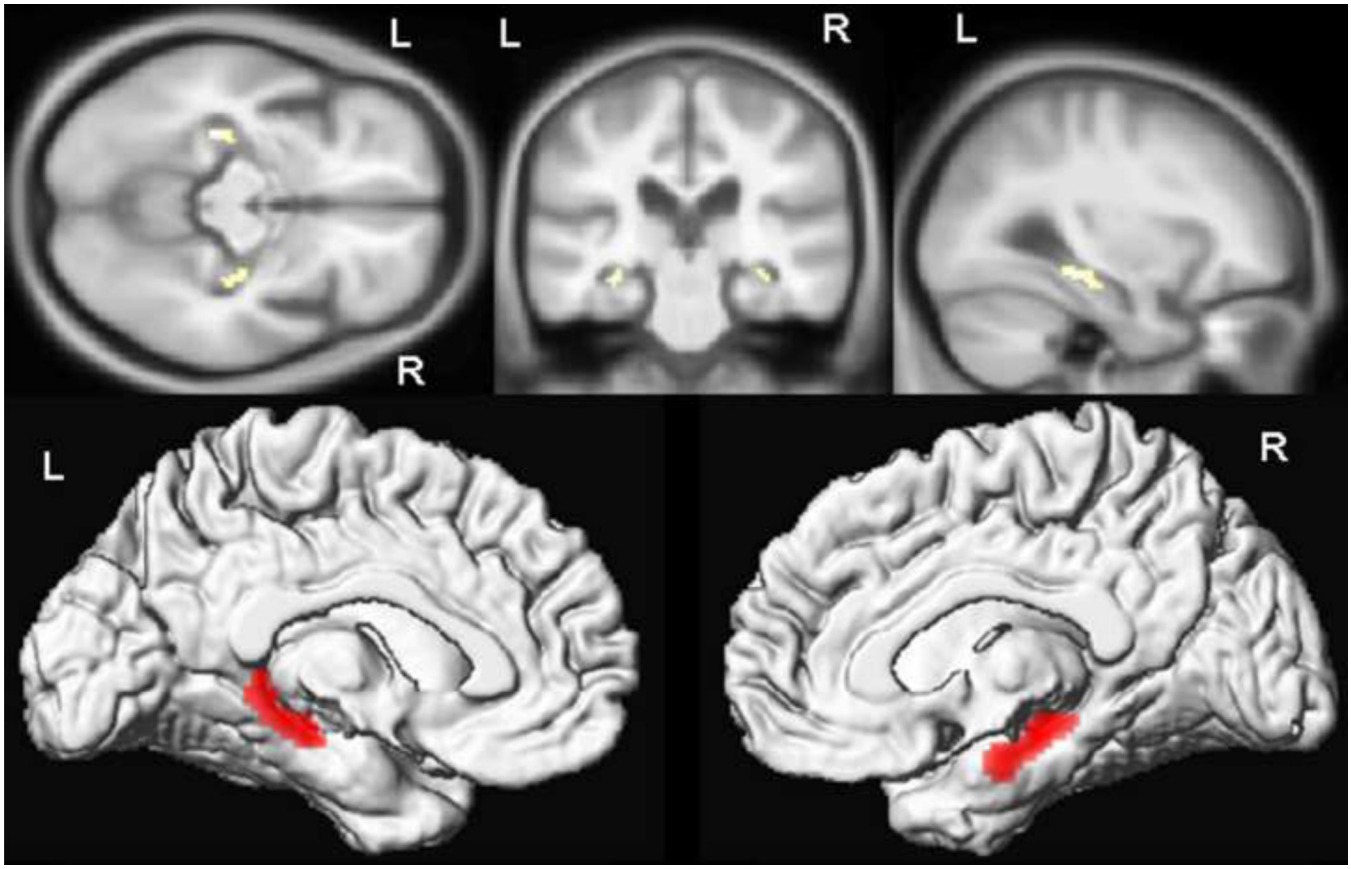


**Figure 1. Voxel-based morphometry comparing DLB and AD**

Voxel-based analysis shows the differences in grey matter density among patients with DLB and AD. Patients with AD had reduced grey matter density ($p<.05$; using family-wise error correction for multiple comparisons) in both hippocampi compared to DLB (shown in yellow on the custom template sections and in red on the surface-render images). On the left side, the differences were more prominent in the posterior portion of the hippocampus.

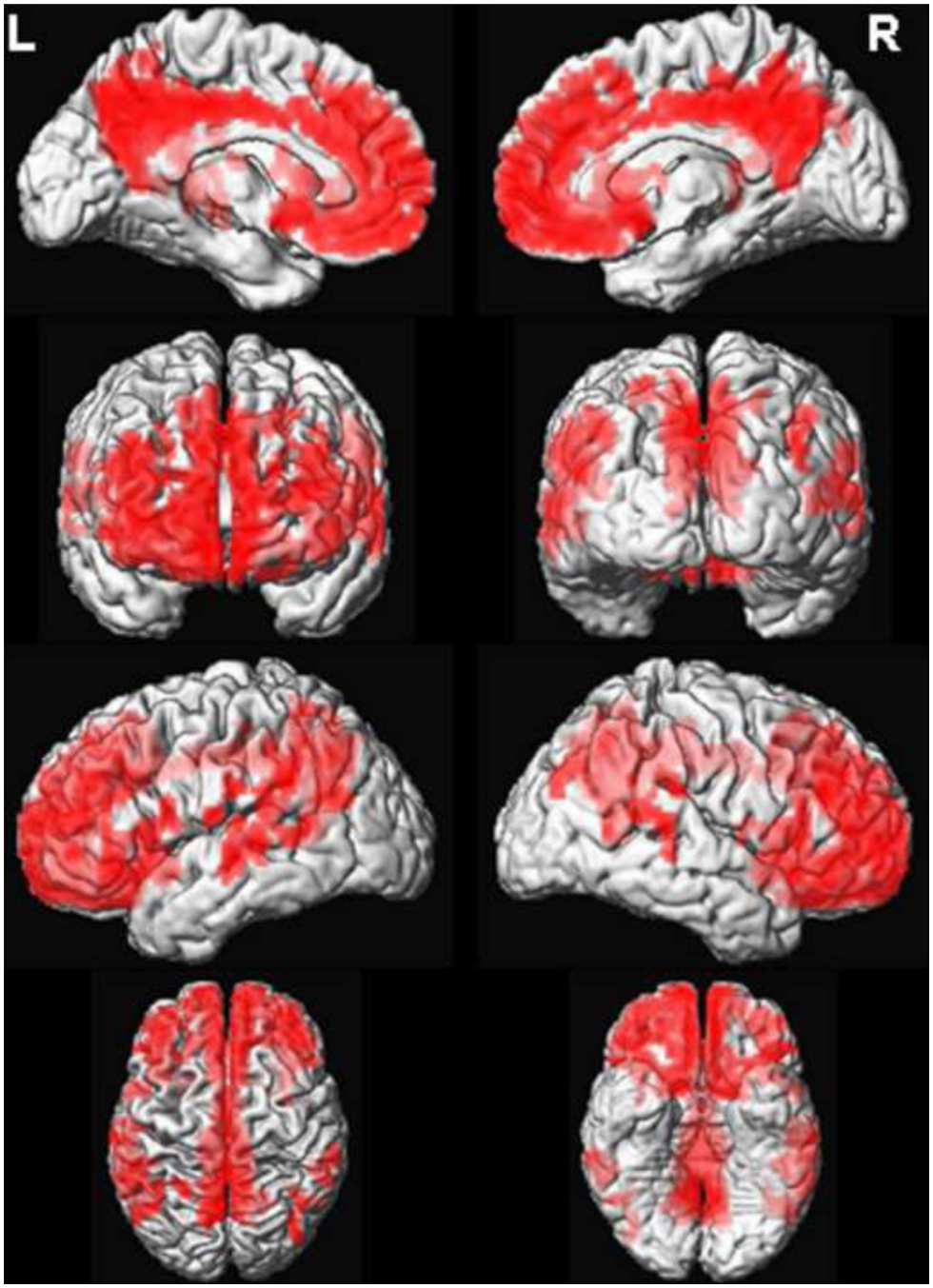


**Figure 2. Regional PiB retention in patients with DLB**

Regional distribution of PiB retention in PiB-positive DLB patients (n=11) were compared to PiB negative CN subjects (n=33). PiB retention was increased ($p<0.05$; using family-wise error correction for multiple comparisons) in the frontal, parietal and superior temporal lobe association cortices (shown in red on the surface-render images). Inferior and medial temporal lobes, occipital lobes and pre and postcentral gyri were typically spared in patients with DLB who were PiB-positive.

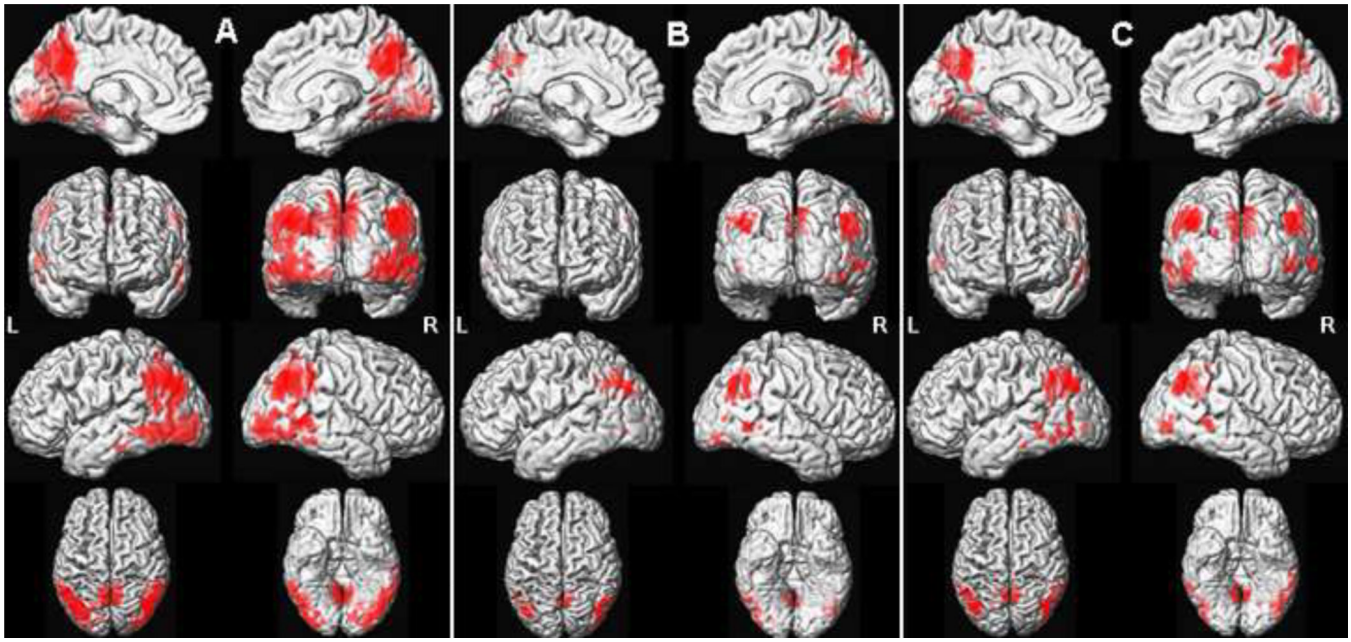


**Figure 3. Regional FDG hypometabolism in patients with DLB**

Regional FDG hypometabolism in patients with DLB (n=21) compared to CN subjects (n=42) involves the occipital and posterior temporoparietal lobes (shown in red on the surface-render images) (**A**). A similar pattern of FDG hypometabolism is present in PiB-negative DLB patients (n=10) compared to PiB-negative CN subjects (n=33)(**B**) and in PiB-positive DLB patients (n=11) compared to PiB-negative CN subjects (**C**) ($P < 0.05$; using family-wise error correction for multiple comparisons). While the patterns of hypometabolism are similar, the extent and the significance of these differences rank with the sample size. The patterns of FDG hypometabolism among the three comparisons can be replicated by varying the p-value thresholds (data not-shown).

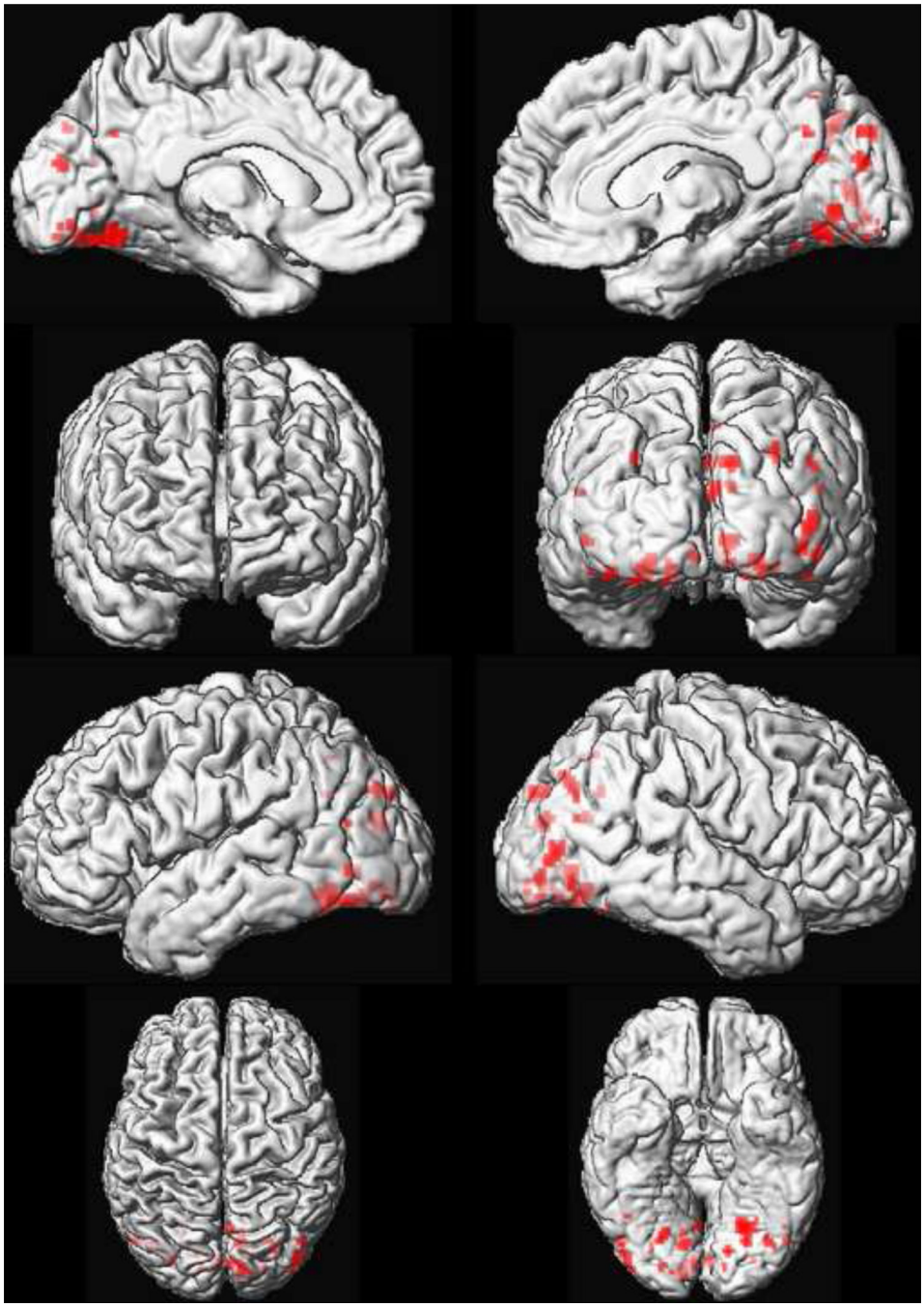

**Figure 4. Regional FDG hypometabolism in patients with DLB compared to AD**

Patients with DLB had lower metabolism ($p<0.05$; using family-wise error correction for multiple comparisons) in the occipital lobe, posterior temporoparietal lobes compared to patients with AD (shown in red on the surface-render images).

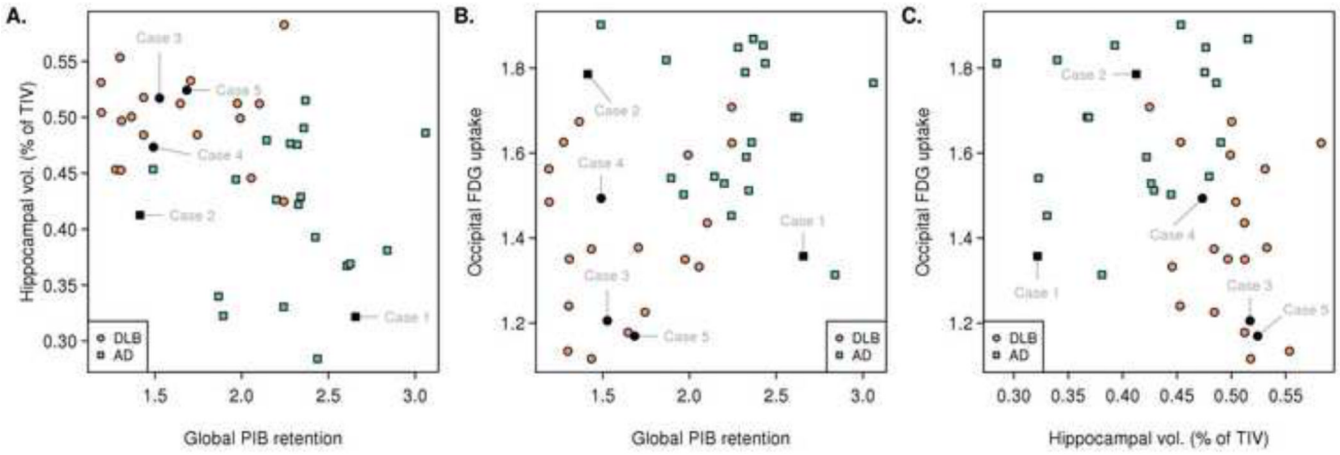


**Figure 5. Distinguishing patients with DLB from AD using two imaging markers**

The plots show distribution of the hippocampal volumes and global PiB retention (**A**); occipital lobe FDG uptake and global PiB retention (**B**); hippocampal volumes and occipital lobe FDG uptake (**C**) in patients with DLB (orange circles) and AD (green squares). The cases with autopsy confirmation (table 3) are labeled on the plots in black. Case 2 was diagnosed as AD antemortem, but had argyrophilic grain disease of the hippocampus on pathological examination. Although there is an overlap between patients with AD and DLB for each of the imaging markers, the groups are separated better with two imaging markers than a single imaging marker.

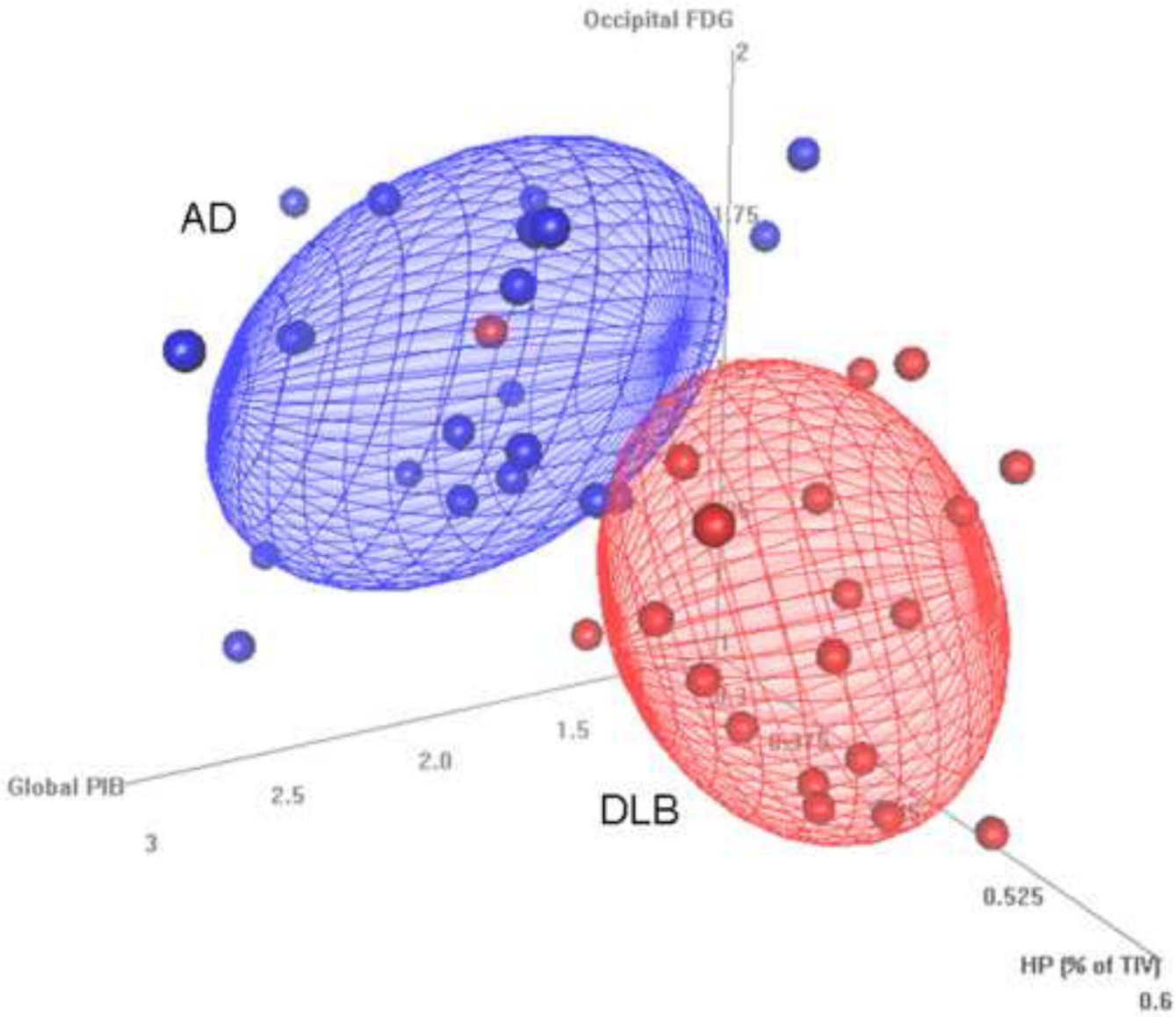


**Figure 6. Three dimensional view of the imaging variables in patients with AD and DLB**

Red plots represent the DLB subjects while blue plots represent the AD subjects. Observations that appear larger represent data points that are closer to the viewer. The ellipsoids for the two groups are concentration ellipsoids. For each group, assuming normality, the dimensions have been set to contain half of the expected values. Except for one DLB patient, all AD and DLB patients are separated using multimodality imaging measures.

## Table 1

Patient characteristics

| Characteristic | CN (*n* = 42) | DLB (*n* = 21) | AD (*n* = 21) | *P*-value[a] |
|---|---|---|---|---|
| Gender, no. (%) | | | | 1.00 |
| Women | 6 (14) | 3 (14) | 3 (14) | |
| Men | 36 (86) | 18 (86) | 18 (86) | |
| Age, years, median (min., max.) | 74 (59, 87) | 73 (60, 87) | 77 (58, 92) | 0.30 |
| Education, years, median (min., max.) | 15 (12, 20) | 15 (8, 20) | 16 (12, 20) | 0.96 |
| MMSE, median (min., max.) | 29 (27, 30) | 22 (6, 29) | 21 (6, 28) | 0.80 |
| CDR sum of boxes, median (min., max.) | 0 (0, 0) | 5 (1, 17) | 5 (1, 13) | 0.56 |
| Total UPDRS, median (min., max.)[b] | 0 (0, 4) | 12 (0, 23) | 0 (0, 11) | <0.001 |

CDR: Clinical Dementia Rating; MMSE: Mini Mental State Examination; UPDRS: Unified Parkinson's Disease Rating Scale

[a] Based on chi-squared test of all groups for gender; based on three-sample Kruskal-Wallis for age and education; based on Wilcoxon rank-sum/Mann-Whitney U test comparing DLB to AD for MMSE and CDR sum of boxes

[b] Missing for 1 CN and 1 AD patient.

## Table 2

Logistic regression model summaries for distinguishing DLB from AD patients

| | | *P*-value[a] | | |
|---|---|---|---|---|
| **Model** | **AUROC / C-statistic** | **PIB** | **FDG** | **Hipp.** |
| Single modality | | | | |
| PIB | 0.89 | <0.001 | | |
| FDG | 0.84 | | 0.001 | |
| MRI | 0.89 | | | 0.002 |
| Two modalities | | | | |
| PIB + FDG | 0.94 | 0.003 | 0.01 | |
| PIB + MRI | 0.96 | 0.007 | | 0.02 |
| FDG + MRI | 0.96 | | 0.01 | 0.008 |
| All three modalities | 0.98 | 0.05 | 0.04 | 0.04 |

[a]Based on Wald test.

**Table 3**

Imaging and pathologic findings in five autopsy confirmed cases

| | Clinical diagnosis | Age at imaging | Imaging to autopsy period (mo.) | Hippocampal volume /TIV | Global PiB retention ratio | Occipital FDG uptake | Pathologic diagnosis | LRP | Braak NFT stage | Neuritic plaques |
|---|---|---|---|---|---|---|---|---|---|---|
| **Case 1** | Probable AD | 82 | 10 | 0.32 | 2.66 | 1.36 | AD (high likelihood) | None | VI | Frequent |
| **Case 2** | Probable AD | 88 | 11 | 0.41 | 1.41 | 1.79 | AD (low likelihood)* | None | II | Sparse |
| **Case 3** | Probable DLB | 81 | 11 | 0.52 | 1.53 | 1.21 | LBD (high likelihood) | Limbic (Transitional) | III | Sparse |
| **Case 4** | Probable DLB | 75 | 17 | 0.47 | 1.49 | 1.49 | LBD (high likelihood) | Diffuse (Neocortical) | II | Moderate |
| **Case 5*** | Probable DLB | 75 | 18 | 0.52 | 1.68 | 1.17 | LBD (high likelihood) | Diffuse (Neocortical) | III | Sparse |

TIV = total intracranial volume; LRP = Lewy-related pathology; NFT = neurofibrillary tangle

*Argyrophilic grain disease in the hippocampus.